ON THE COMPUTATION OF STREAM FUNCTIONS FROM THE WIND FIELD

HARRY F. HAWKINS and STANLEY L. ROSENTHAL

National Hurricane Research Laboratory, U.S. Weather Bureau, Miami, Fla.

ABSTRACT

In most tropical regions, the large-scale flow patterns are most reliably established by analysis of the wind reports. In these regions, stream functions must be calculated either wholly or partially from the wind analysis itself. To do this, however, it is necessary to specify the stream function, or its normal derivative, on the boundary of the region considered. This paper examines several schemes which may be useful for this purpose.

1. INTRODUCTION

The Helmholtz theorem,

$$\mathbf{V} = \mathbf{k} \times \nabla\psi + \nabla\chi \tag{1}$$

which allows decomposition of the wind vector into non-divergent and irrotational components, has proven to be a useful meteorological tool. (V is the horizontal wind, k is a unit-vertical vector, ψ is the horizontal stream function, ∇ is the isobaric gradient operator, and χ is the horizontal velocity potential.) Most applications of equation (1) have been to middle- and high-latitude data within the framework of numerical weather prediction models. Under these circumstances, ψ is usually computed from the pressure-geopotential by use of a wind-pressure relationship. The velocity potential is then obtained from a second diagnostic calculation in which the thermodynamic and vorticity equations, and the wind-pressure equation, are employed. In such a procedure, wind observations serve only as an aid in the analysis of the geopotential field and are discarded thereafter.

In most tropical areas, however, the synoptic-scale flow pattern is most reliably established by the wind reports themselves. Thus, in applications of equation (1) to low latitudes, it would seem reasonable to compute ψ directly from the wind field. The vertical component of the curl of equation (1) is

$$\nabla^2\psi = \mathbf{k} \cdot \nabla \times \mathbf{V} \equiv \zeta \tag{2}$$

which may be solved as a Poisson equation for ψ if ζ is computed from the wind analysis.

2. THE PROBLEM

To solve equation (2), it is necessary to know ψ or its normal derivative on the boundary of the region over which the solution is to be valid. In a previous paper [1], the boundary values of ψ were established as follows. If

s is distance on the earth along the boundary, positive in the counterclockwise sense, $\mathbf{n}$ is a unit vector normal to the boundary pointing outward, and n is distance on the earth normal to the boundary increasing outward, then the scalar product of $\mathbf{n}$ with equation (1) gives

$$(\partial\psi/\partial s) = -v_n + (\partial\chi/\partial n) \tag{3}$$

where v_n, the velocity component normal to the boundary, is the only term known from the wind analysis. Integration of (3) around the boundary curve yields

$$\oint v_n ds = \oint (\partial\chi/\partial n)\, ds \equiv \overline{(\partial\chi/\partial n)}\, S \tag{4}$$

where S is the total length of the boundary. In [1], equation (3) was replaced by

$$(\partial\psi/\partial s) = -v_n + \overline{(\partial\chi/\partial n)} \tag{5}$$

and the wind components normal to the boundary were replaced by $v_n - \overline{(\chi\partial/\partial n)}$. This has the effect of reducing the mean divergence over the area enclosed by the boundary curve to zero. If one of the boundary-grid points is assigned an arbitrary value of ψ, the stream function at the remaining boundary-grid points may be found by numerical integration of (5) along the boundary. This technique appears to be entirely equivalent to that employed by Brown and Neilon [2] in an application to middle-latitude data. For the cases treated in [2] and also for those utilized in [1], the method described above appeared to give satisfactory results.

In later applications of the same technique by Bedient and Vederman [3] and by Hawkins (research in progress at the National Hurricane Research Laboratory), it was found that utilization of equations (4) and (5) leads to difficulties which can best be described by the following example taken from Hawkins' work. Figure 1 shows a superimposition of Hawkins' grid on the Mercator projection he uses. There are 10 rows and 13 columns; spacing between grid points is the length of 2° of longitude
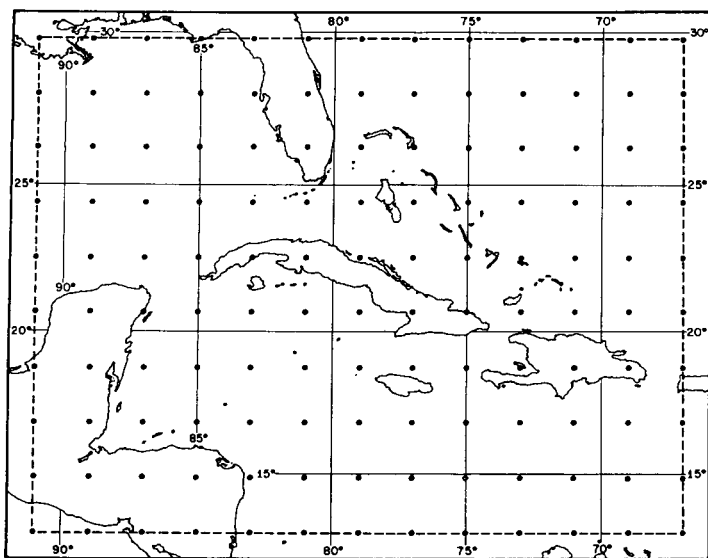
FIGURE 1.—Region of study and grid points. The heavy border in figures 2–15 outlines this same region.
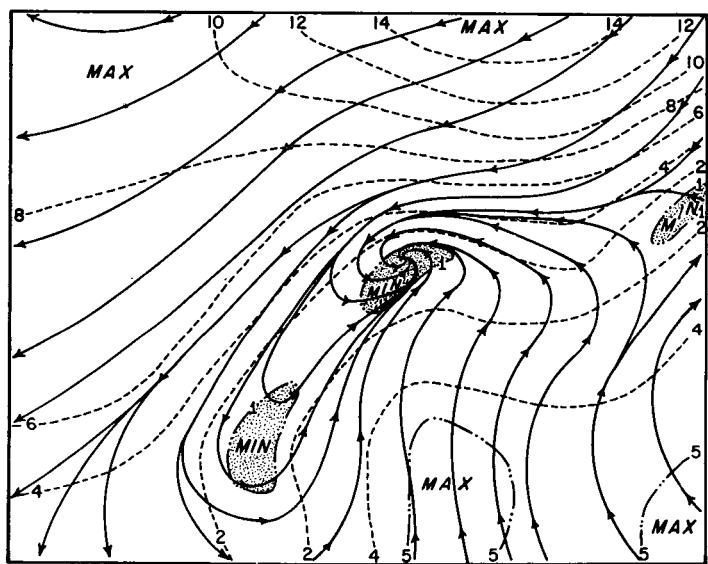

FIGURE 2.—Wind analysis at 1000 mb. for 1500 GMT, October 13, 1956. Streamlines are solid lines with arrows. Isotachs are dashed lines. Wind speeds are given in m. sec.$^{-1}$
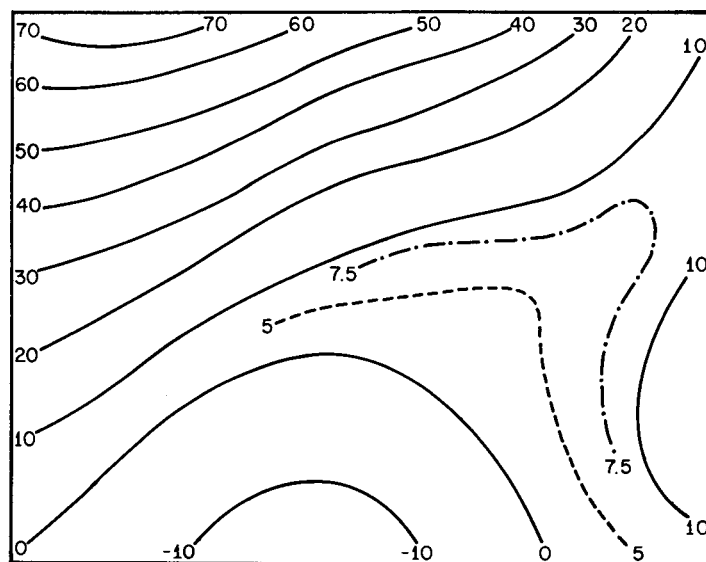

FIGURE 3.—The stream function at 1000 mb. for 1500 GMT, October 13, 1956, obtained from the original calculation in which equations (4) and (5) are used to establish the boundary conditions on ψ. To obtain stream function values in m.^{2} sec.$^{-1}$, multiply by 2×10^5. Stream function values given by the figure may be thought of as pressure heights in meters. The non-divergent wind can be calculated by use of the geostrophic-wind equation, using 5×10^{-5} sec.$^{-1}$ for the Coriolis parameter and 10 m. sec.$^{-2}$ for gravity.

distorted picture of the cyclonic system. The latter appears as an open wave in the easterlies with lowest ψ-values on the southern boundary. Details of the calculation are as follows. The integrations of equations (4) and (5) were done by the trapezoidal rule; the vorticity was approximated by

$$\zeta_{i,j} \approx (m_i/2\Delta s)[v_{i,j+1} - v_{i,j-1} - u_{i+1,j} + u_{i-1,j}]$$

where i is the row (meridional) index and j is the column (longitudinal) index, v is the meridional wind component, u is the zonal wind component, m is the map-scale factor, and Δs is the mesh constant; the Laplacian was approximated by

$$(\nabla^2 \psi)_{i,j} = (m_i^2/\Delta s^2)[\psi_{i+1,j} + \psi_{i-1,j} + \psi_{i,j+1} + \psi_{i,j-1} - 4\psi_{i,j}]$$

and the resulting system of algebraic equations was solved for $\psi_{i,j}$ by Liebmann relaxation with a tolerance of 60,000 m.^{2} sec.$^{-1}$

It may be argued that, even aside from truncation errors, the stream function cannot provide a close fit to the wind analysis because the winds are not non-divergent. As will be seen later, this argument has a certain degree of validity. However, it would indeed be disappointing if a closer correspondence between the wind analysis and the stream function could not be obtained. Figures 4 and 5 show, respectively, the vorticity and divergence

$$(\nabla \cdot \mathbf{V})_{i,j} \approx (m_i/2\Delta s)(u_{i,j+1} - u_{i,j-1} + v_{i+1,j} - v_{i-1,j})$$
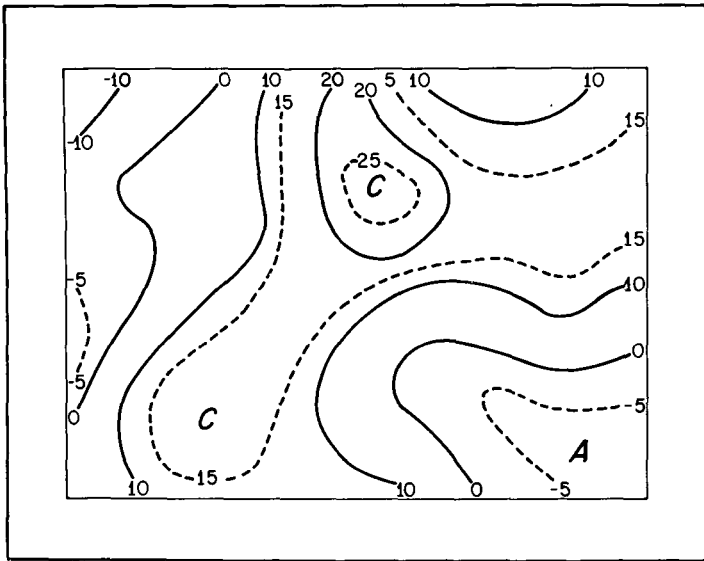
at 22.5°N. (the true latitude of the projection). Figure 2 shows the subjective analysis of the 1000-mb. streamlines and isotachs for 1500 GMT, October 13, 1956. Of particular interest is the cyclone in the center of the grid and the trough which protrudes southwestward from the cyclone.

Figure 3 shows the stream function which results when equations (4) and (5) are used to establish the boundary values of ψ^1. Notice that the stream function gives a

---

[1] This calculation proceeded as follows. Grid-point winds were read from figure 2. The relative vorticity was computed at each internal grid point. Boundary values of ψ were calculated from equation (5). Equation (2) was solved for the stream function.

FIGURE 4.—Relative vorticity at 1000 mb. for 1500 GMT, October 13, 1956, in units of 10^{-6} sec.$^{-1}$
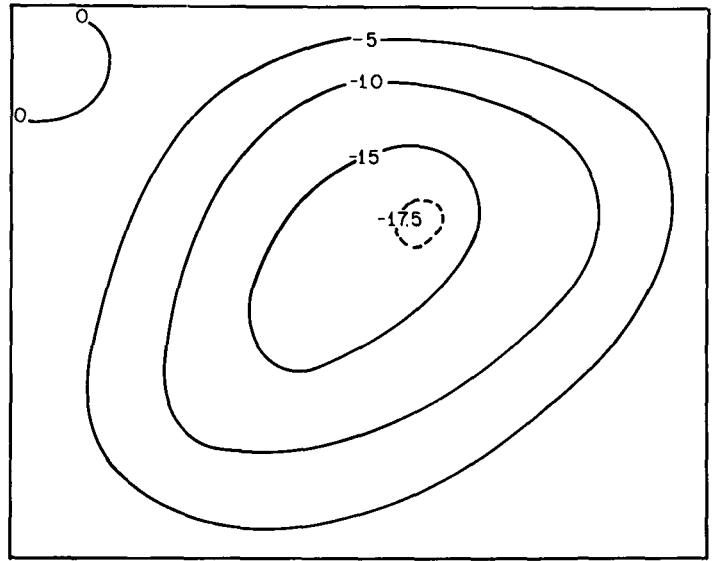

FIGURE 6.—Partial stream function (ψ_{R1}) at 1000 mb. for 1500 GMT, October 13, 1956, calculated from equation (7). Units and scaling are the same as in figure 3.

FIGURE 5.—Divergence at 1000 mb. for 1500 GMT, October 13, 1956, in units of 10^{-6} sec.$^{-1}$

FIGURE 7.—Partial stream function (ψ_{R2}) at 1000 mb. for 1500 GMT, October 13, 1956, calculated from equation (8). Units and scaling are the same as in figure 3.
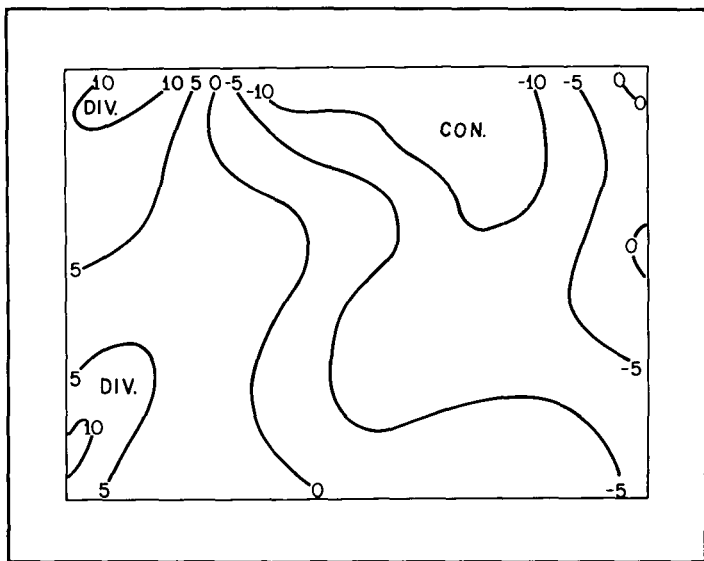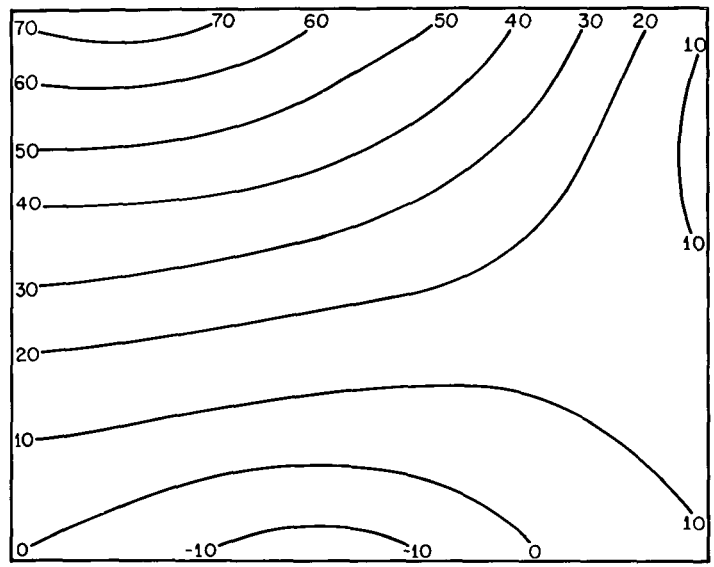
computed from the wind analysis. Clearly, the vorticity, on the average, is significantly larger in magnitude than is the divergence and one would not want the χ-field to be of sufficient intensity to explain the major differences between the flow patterns portrayed by figures 2 and 3.

A clue to the nature of the difficulty is provided by the following analysis. Let ψ_B be the boundary values of ψ calculated from equations (4) and (5). If ψ_R is used to represent the stream function shown by figure 3, then

$$\psi_R = \psi_{R1} + \psi_{R2} \tag{6}$$

where

$$\nabla^2 \psi_{R1} = \zeta, \qquad \psi_{R1} = 0 \text{ on the boundary} \tag{7}$$

and

$$\nabla^2 \psi_{R2} = 0, \qquad \psi_{R2} = \psi_B \text{ on the boundary} \tag{8}$$

The fields of ψ_{R1} and ψ_{R2} are shown, respectively, by figures 6 and 7. From figure 6, we see that the vorticity defines a large cyclone whose center is, more or less, in the location of the vortex shown by figure 2. However, ψ_{R2} (fig. 7), which is determined by the boundary conditions, shows relatively strong easterlies along the southern por-

tion of the ψ_{R1}-cyclone and the sum of the two fields gives the open wave shown by figure 3. It therefore appears that at least part of the difficulty lies in the choice of boundary conditions.

Sangster [4] proposes a more rigorous approach to the calculation of boundary values of ψ. This is based on the use of equation (3) in unmodified form. The boundary values of $\partial\chi/\partial n$, needed in equation (3), are calculated from the χ-field obtained from the solution of

$$\nabla^2\chi=\nabla\cdot V, \qquad \chi=0 \text{ on the boundary} \qquad (9)$$

where $\nabla\cdot V$ is the divergence calculated from the wind analysis. Sangster [4] shows that the use of (9) to establish χ maximizes the portion of the total kinetic energy carried by ψ and minimizes the portion carried by χ.

We have experimented with Sangster's method in three versions which differ only in the details of the numerical calculation.

Version I. Equation (9) is solved. $\partial\chi/\partial n$ on the boundary is calculated from a one-sided inward difference over a single grid increment. Equation (3) is integrated trapezoidally along the boundary to obtain boundary values of ψ. Equation (2) is solved to obtain the internal values of ψ.

Version II. Equation (9) is solved. $\partial\chi/\partial n$ is evaluated by centered differences at the grid points adjacent to the boundary (which form what we will call the "inner boundary"). Equation (3) is integrated trapezoidally along the inner boundary and equation (2) is solved for ψ at grid points internal to the inner boundary. To establish ψ on the outer boundary, we take the scalar product of **s** with equation (1). This gives

$$(\partial\psi/\partial n)=v_s-(\partial\chi/\partial s) \qquad (10)$$

which is integrated trapezoidally from the inner to the outer boundary with $\partial\chi/\partial s$ evaluated by centered differences. This establishes ψ at all grid points on the outer boundary with the exception of the four corner points. The corner points are evaluated as simple arithmetic means of the ψ-values at the two adjacent grid points on the outer boundary.

Version III. The stream function on the inner boundary is obtained by the procedure used in Version II. However, before the solution of equation (2) is begun, values for ψ on the outer boundary are calculated by the method used in Version II. At this point, the ψ-values on the inner boundary are discarded and (2) is solved for ψ at grid points internal to the outer boundary.

A calculation using a normal-derivative boundary condition was also carried out.

Normal-Derivative Boundary Condition. Equation (9) is solved for χ. Equation (2) is solved for ψ at grid points internal to the outer boundary; during each scan of the relaxation ψ on the outer boundary is recalculated by a trapezoidal integration of (10) from the inner to the outer
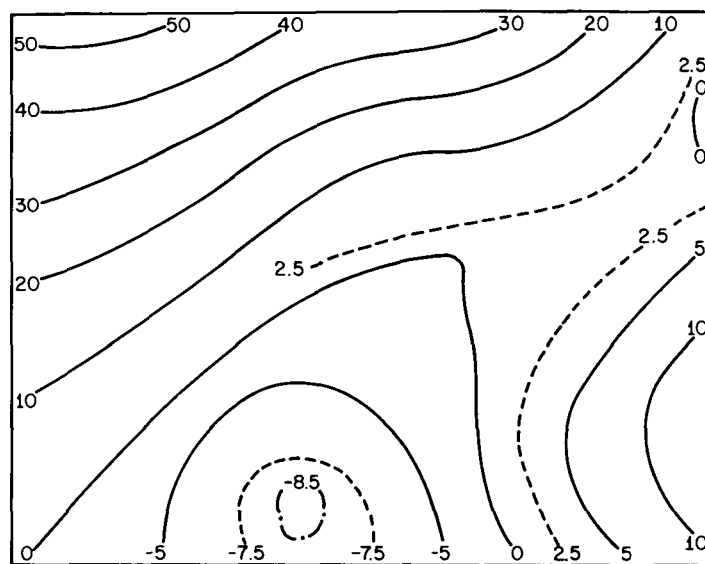

FIGURE 8.—Stream function at 1000 mb. for 1500 GMT, October 13, 1956, calculated by Version I. Units and scaling are the same as in figure 3.

boundary; the most recent estimates of ψ at the internal grid points and a centered difference estimate of $\partial\chi/\partial s$ are used in this calculation.

A version of the approach suggested by Bedient and Vederman [3] was also tested. With the normal-derivative boundary condition, the problem may be stated

$$\nabla^2\psi=\zeta \text{ with } (\partial\psi/\partial n)=v_s-(\partial\chi/\partial s) \text{ on the boundary} \qquad (11)$$

The problem defined by (11) is equivalent to

$$\nabla^2\psi_1=\zeta \text{ with } \psi_1=0 \text{ on the boundary} \qquad (12)$$

$$\nabla^2\psi_2=0 \text{ with } (\partial\psi_1/\partial n)+(\partial\psi_2/\partial n)$$
$$=v_s-(\partial\chi/\partial s) \text{ on the boundary} \qquad (13)$$

where

$$\psi=\psi_1+\psi_2 \qquad (14)$$

Since $\nabla\psi_2$ is a non-divergent vector, we may write

$$\mathbf{k}\times\nabla\psi_3\equiv\nabla\psi_2 \qquad (15)$$

From (15) and (13), we obtain

$$\nabla^2\psi_3=0 \text{ with } (\partial\psi_3/\partial s)$$
$$=(\partial\psi_1/\partial n)-v_s+(\partial\chi/\partial s) \text{ on the boundary} \qquad (16)$$

From (1) and (15), we find

$$(\partial\psi_3/\partial n)=-v_n+(\partial\chi/\partial n) \qquad (17)$$

From equation (15),

$$(\partial\psi_2/\partial s)=(\partial\psi_3/\partial n) \qquad (18)$$

and

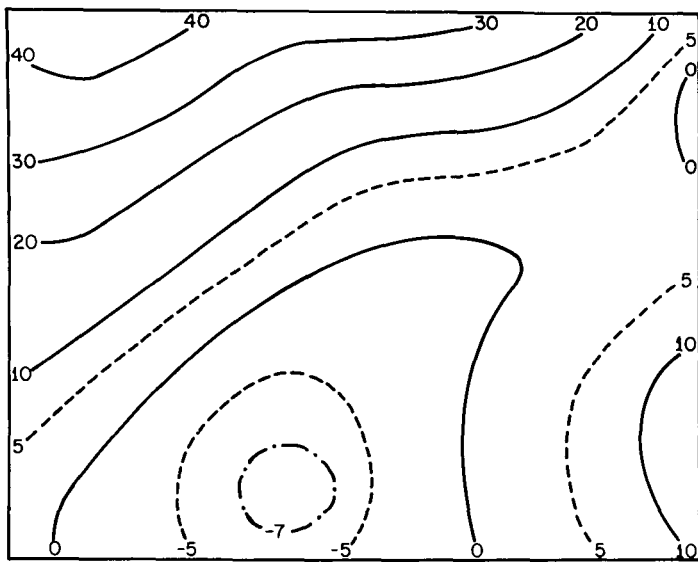$$(\partial\psi_2/\partial n)=-(\partial\psi_3/\partial s) \qquad (19)$$

FIGURE 9.—Stream function at 1000 mb. for 1500 GMT, October 13, 1956, calculated by Version II. Units and scaling are the same as in figure 3.
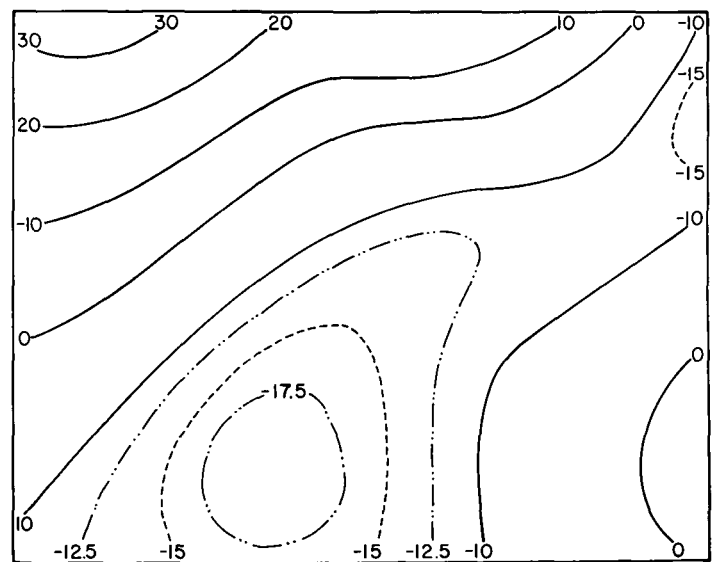

FIGURE 11.—Stream function at 1000 mb. for 1500 GMT, October 13, 1956, calculated with normal-derivative boundary condition. Units and scaling are the same as in figure 3.
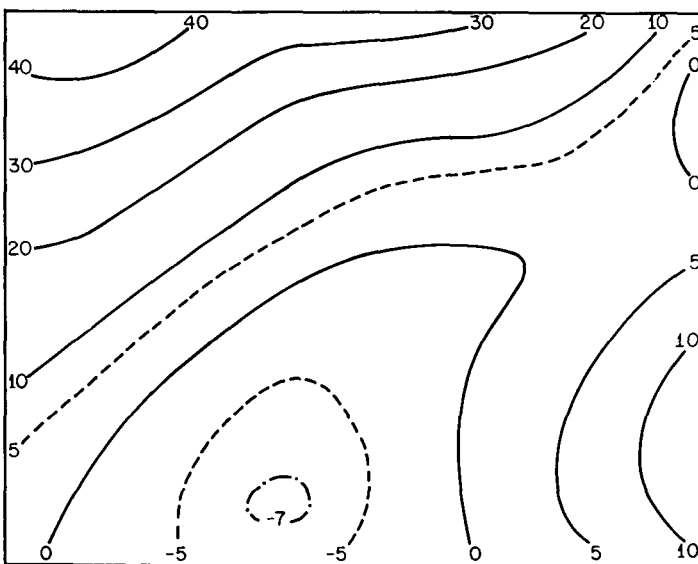

FIGURE 10.—Stream function at 1000 mb. for 1500 GMT, October 13, 1956, calculated by Version III. Units and scaling are the same as in figure 3.
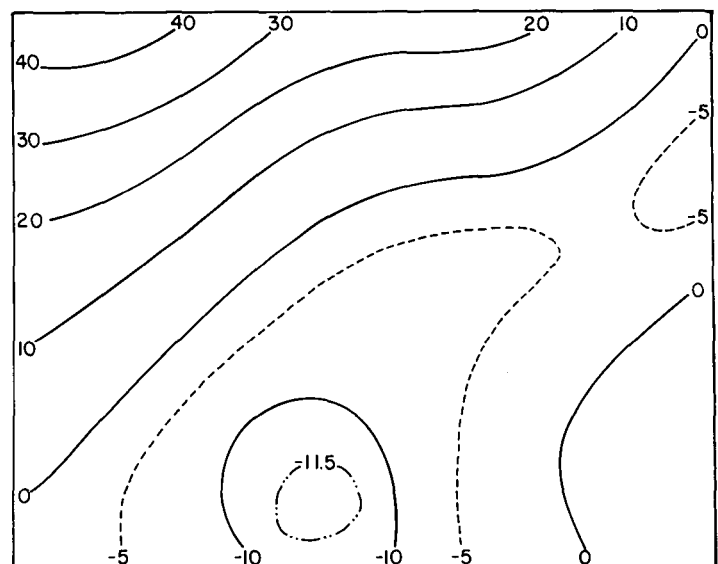

FIGURE 12.—Stream function at 1000 mb. for 1500 GMT, October 13, 1956, calculated from ψ_3-version. Units and scaling are the same as in figure 3.

By use of (12) to (19), the following technique was devised.

ψ_3-*Version*. Equation (9) is solved for χ. Equation (12) is solved for ψ_1. The boundary condition given with (16) is integrated trapezoidally along the inner boundary with $\partial\psi_1/\partial n$ evaluated by centered differences. Equation (17) is integrated trapezoidally from the inner to the outer boundary to establish ψ_3 at all but the corner-grid points on the outer boundary. At the corner points, ψ_3 is taken as the arithmetic mean of the values at the two adjacent outer boundary grid points. The Laplace equation for ψ_3 is solved to obtain values at grid points internal to the outer boundary. Equation (18) with $\partial\psi_3/\partial n$ evaluated

by centered differences is integrated trapezoidally along the inner boundary thereby establishing ψ_2 on the inner boundary. Equation (19) with $\partial\psi_3/\partial s$ evaluated by centered differences is integrated trapezoidally from the inner to the outer boundary which establishes ψ_2 on the outer boundary with the exception of the corner-grid points. The corner points are treated as described above for ψ_3. The Laplace equation for ψ_2 is solved to obtain values at grid points internal to the outer boundary. Equation (14) is used to calculate ψ.

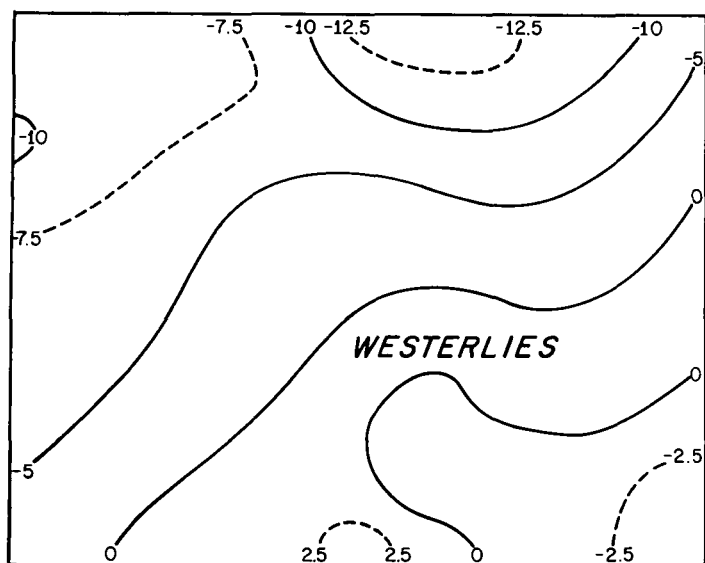Figures 8–12 show the results obtained from the five methods just described. These stream functions appear

FIGURE 13.—Zonal-wind component at 1000 mb. for 1500 GMT, October 13, 1956, calculated from wind analysis shown by figure 2. Units are m. sec.$^{-1}$; west winds are positive.
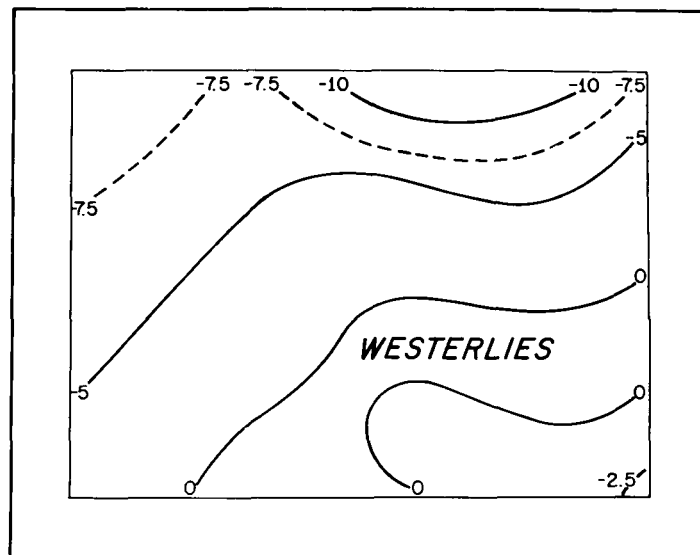

FIGURE 14.—Zonal-wind component at 1000 mb. for 1500 GMT, October 13, 1956, calculated from equation (20) using the stream function obtained from Version III. Units are m. sec.$^{-1}$; west winds are positive.

to give somewhat better representations of the flow pattern than was the case with the original calculation. The patterns are, however, still distorted. None of the methods gives a vortex in the location shown by figure 2. On the other hand, all of the methods give a spurious cyclone close to the southern boundary.

To pursue the matter further, figure 13 shows the zonal component of the analyzed wind. In particular, we wish to draw attention to the undulating zone of westerlies found over the southern portion of the chart. These westerlies constitute the flow around the southern portions of the cyclone and trough. For the sake of comparison, figure 14 shows the zonal wind computed from

$$u = -(\partial\psi/\partial y) + (\partial\chi/\partial x) \tag{20}$$

where the stream function obtained from Version III has been employed. Here we note a zone of westerlies which in shape and location is quite similar to that in figure 13. Finally, figure 15 shows the zonal wind computed from

$$u = -(\partial\psi/\partial y) \tag{21}$$

where, again, the stream function obtained from Version III has been used. The zonal winds of figure 15 show a break in the westerly band in the region where the flow around the southern portion of the cyclone should be. The easterlies which occupy this region close off the spurious cyclone noted near the southern boundary on the stream function charts. Thus we must conclude that accurate portrayal of the wind directions associated with the cyclone and trough found on figure 2 requires both the irrotational and the non-divergent parts of the wind if the calculations are carried out by the techniques employed here.

Root-mean-square-vector-errors (RMSVE) appropriate to each calculation are shown in table 1. It is clear that the original calculation and Version I are decidedly inferior to the other techniques. Versions II and III and the normal-derivative calculation give the best fits if we compare the analyzed wind to the stream wind alone. If we compare with the sum of the stream and potential winds, Versions II and III are somewhat more accurate than the normal derivative calculation. Reduction of the relaxation tolerance from 60,000 m.^{2} sec.$^{-1}$ to 6,000 m.^{2} sec.$^{-1}$ resulted in changes in the RMSVE of about 10^{-3} sec.$^{-1}$.

Tables 2–6 show similar statistics for other cases taken from the data files at the National Hurricane Research Laboratory. For all of these cases, the geographical area and the grid are very nearly the same as those shown by figure 1. Overall it seems that the original calculation is clearly inferior to the other techniques. Versions II and III and the normal-derivative calculations seem to be the most accurate of the methods tested. However, the com-

TABLE 1.—RMSVE (m. sec.$^{-1}$) for 1000 mb., 1500 GMT, October 13, 1956

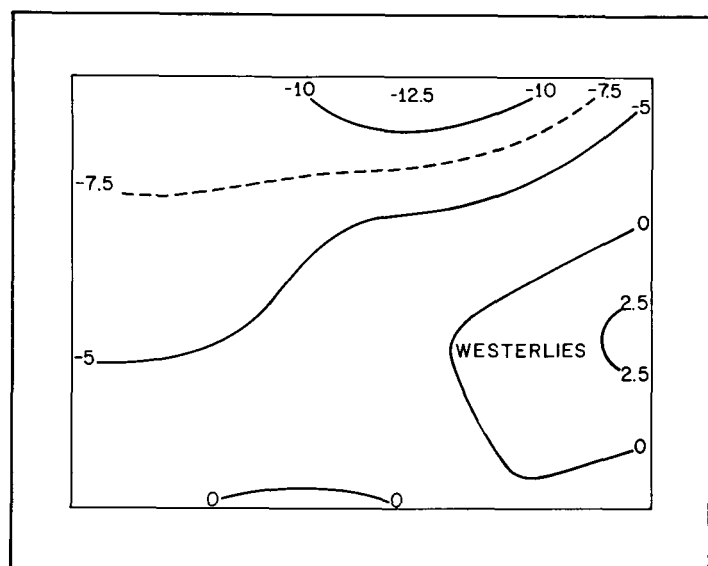| Comparison / Method	Analyzed wind against $k\times\nabla\psi$	Analyzed wind against $k\times\nabla\psi+\nabla\chi$
Original	4.01	3.35
Version I	2.12	.97
Version II	1.80	.43
Version III	1.79	.40
Normal derivative	1.78	.53
ψ_3	1.87	.53

FIGURE 15.—Zonal component of the non-divergent wind at 1000 mb. for 1500 GMT, October 13, 1956, calculated from equation (21) using the stream function obtained from Version III. Units are m. sec.$^{-1}$; west winds are positive.

putations with the normal-derivative boundary condition required about twice the number of relaxation scans as did Versions II and III. On this basis, Versions II and III appear to be the most useful of the techniques tested.

3. SUMMARY AND CONCLUSIONS

Calculations of boundary values of the stream function by the crude technique which makes use of equations (4) and (5) cannot be relied upon to give satisfactory results for regions of the size considered here. In view of the somewhat disappointing results obtained by Bedient and Vederman [3] (whose calculations covered the area, 20° S.–35° N., 105° E. eastward to 145° W.) in an application of equations (4) and (5), it seems that this problem is also encountered when larger regions are considered.

Substantially better solutions for ψ are obtained by use of the boundary condition given by equation (3) or by that given with equation (11), provided that the derivatives of the velocity potential are estimated as centered differences of the solution to (9). Solution of the problem with the

normal-derivative boundary condition (equation (11)) requires about twice as much machine time as do the techniques based on equation (3). This is the result of a slower convergence rate in the relaxation.

It is not unlikely that other schemes, such as Sangster's [4] staggered lattice technique, would prove to be more accurate than any of those tested here.

TABLE 3.—RMSVE (m. sec.$^{-1}$) for 850 mb., 0000 GMT, August 25, 1962

Comparison Method	Analyzed wind against $k\times\nabla\psi$	Analyzed wind against $k\times\nabla\psi+\nabla\chi$
Original	0.95	0.77
Version I	.73	.54
Version II	.72	.55
Version III	.72	.55
Normal derivative	.70	.53
ψ_3	1.13	1.03

TABLE 4.—RMSVE (m. sec.$^{-1}$) for 850 mb., 0000 GMT, August 26, 1962

Comparison Method	Analyzed wind against $k\times\nabla\psi$	Analyzed wind against $k\times\nabla\psi+\nabla\chi$
Original	1.15	0.75
Version I	.97	.48
Version II	.98	.52
Version III	.97	.50
Normal derivative	.95	.47
ψ_3	1.12	.77

TABLE 5.—RMSVE (m. sec.$^{-1}$) for 250 mb., 0000 GMT, August 25, 1962

Comparison Method	Analyzed wind against $k\times\nabla\psi$	Analyzed wind against $k\times\nabla\psi+\nabla\chi$
Original	2.13	1.81
Version I	1.50	1.11
Version II	1.12	.69
Version III	1.10	.65
Normal derivative	1.07	.64
ψ_3	1.16	.75

TABLE 2.—RMSVE (m. sec.$^{-1}$) for 850 mb., 1500 GMT, October 13, 1956

Comparison Method	Analyzed wind against $k\times\nabla\psi$	Analyzed wind against $k\times\nabla\psi+\nabla\chi$
Original	2.65	1.98
Version I	1.73	.72
Version II	1.65	.68
Version III	1.64	.65
Normal derivative	1.58	.62
ψ_3	1.69	.83

TABLE 6.—RMSVE (m. sec.$^{-1}$) for 250 mb., 0000 GMT, August 26, 1962

Comparison Method	Analyzed wind against $k\times\nabla\psi$	Analyzed wind against $k\times\nabla\psi+\nabla\chi$
Original	1.32	1.11
Version I	1.07	.86
Version II	.83	.77
Version III	.83	.76
Normal derivative	.84	.80
ψ_3	1.02	.79

REFERENCES

1. S. L. Rosenthal, "A Barotropic Model for Prediction in the Tropics," Paper presented at the United States-Asian Military Weather Symposium, John Hay Air Base, Philippine Islands, February 3–7, 1963.

2. J. Brown and J. R. Neilon, "Case Studies of Numerical Wind Analysis," *Monthly Weather Review,* vol. 89, No. 3, March 1961, pp. 83–90.

3. H. A. Bedient, and J. Vederman, "Computer Analysis and Forecasting in the Tropics," *Monthly Weather Review,* vol. 92, No. 12, Dec. 1964, pp. 565–577.

4. W. E. Sangster, "A Method of Representing the Horizontal Pressure Force Without Reduction of Station Pressures to Sea Level," *Journal of Meteorology,* vol. 17, No. 2, Apr. 1960, pp. 166–176.